A SCATTERING MODEL FOR RAIN DEPOLARIZATION*

by

Paris H. Wiley
Warren L. Stutzman
and
C. W. Bostian

of

Virginia Polytechnic Institute and State University
Department of Electrical Engineering
Blacksburg, Virginia 24061

*This research was supported by NASA under Grant NGR-47-004-091.

ABSTRACT

A method is presented for calculating the amount of depolarization caused by precipitation for a propagation path. In the model the effects of each scatterer and their interactions are accounted for by using a series of simplifying steps. It is necessary only to know the forward scattering properties of a single scatterer. For the case of rain the results of this model for attenuation, differential phase shift, and cross polarization agree very well with the results of the only other model available, that of differential attenuation and differential phase shift. In this model the effective percentage of oblate rain drops is easily included in cross-polarization calculations and allows for good agreement with experimental results. Further flexibility is possible if one includes a distribution of drop shapes.

Calculations presented here show that horizontal polarization is more sensitive to depolarization than is vertical polarization for small rain drop canting angle changes. This effect increases with increasing path length.

INTRODUCTION

Prediction of the scattering of electromagnetic waves due to rain is important for communication links at millimeter wavelengths [1]. Rainfall scatter produces both attenuation and depolarization. The problem of attenuation due to rainfall has received considerable theoretical attention [2,3]. But relatively little about depolarization is available in the literature. All computations of the cross-polarization level to date have been based on the differential attenuation-differential phase shift models proposed by Thomas [4] and Watson [5] and attenuation values computed using van de Hulst's method [6]. The differential attenuation-differential phase shift model recognizes that raindrops tend to be oblate spheroids rather than true spheres and, thus, a rain-filled space will attenuate and phase shift waves polarized along the narrow dimension of drop (near vertical) less than waves polarized along the wide dimension of the drop (near horizontal). Depolarization by differential attenuation is illustrated in Figure 1, where E_T represents a transmitted wave which is polarized along neither the vertical axis nor the horizontal axis. E_T can be decomposed into components along the horizontal axis, E_1, and along the vertical axis, E_2. As the wave propagates through a drop E_1 will be attenuated more than E_2, giving E_1' and E_2'. The resultant vector E_R with components E_1' and E_2' is not parallel to E_T and thus has a component perpendicular to it which corresponds to a cross-polarized wave (for the linearly polarized case).

A disadvantage of the differential attenuation-differential phase shift model is that it requires the existence of two preferred polarizations (major and minor axes of the drop) for which signals are not depolarized. Because of the physical symmetry of the individual drops, rain has this property but sleet and snow do not. Hence sleet and snow depolarization cannot be predicted by the differential attenuation-differential phase shift model.

A new model is proposed here which involves summing the forward scattered radiation from each raindrop to obtain the total electric field intensity at the receiver location. Some simplifying steps discussed in the next section allow the summation process to be carried out very easily by computer. There are many variables in a real rain which affect electromagnetic waves, but this model includes only those parameters which are necessary for good agreement with experiment and useful in predicting rain effects on communication links. To this end we have made several assumptions. We assume that the transmit and receive antennas are pointed directly at each other and have dual orthogonal polarizations which are aligned. The rain rate is assumed to be uniform along the entire path. Although real rain contains a statistical distribution of drop sizes we have assumed here that all drops are equal in size to that of the most frequently occurring drop size in the Laws-Parsons distribution [7]. The shape of the drops is assumed to be either that of an oblate spheroid or a sphere. Real rain is known to be a mixture of spherical, oblate, prolate and irregular drops [8]. An effective percentage of oblate drops (with the remainder spherical) is assumed to model the actual rain. All

oblate drops are oriented identically with a canting angle defined as the angle between the major axis of the drop and the horizontal. As a consequence of these assumptions about the rain we may say that the rain-filled space is large-scale homogeneous. It is further assumed that the beamwidths of both the transmitting and receiving antennas are sufficient so that small variations in the beamwidths have negligible effect on the received signal levels. This implies that many Fresnel zones are included in the common volume of the main beams of the antennas. Also the incident and scattered fields are assumed to be spherical waves. In order to carry out a detailed calculation it is necessary to know the forward scattering properties of a single raindrop for the particular frequency of interest.

DEVELOPMENT OF THE MODEL

The exact solution for the scattered field arriving at the receiving antenna would involve summing up the fields scattered off of every raindrop illuminated by the transmitting antenna. Fortunately, it is not necessary to do this. In fact, it is well known that for isotropic antennas the field at the receiver is exactly one-half that found by considering the first Fresnel zone alone. Since we have assumed that there are many Fresnel zones inside the common volume of the antenna mainbeams, the directivity of the antennas will have only a minor effect. Thus we will work with only the first Fresnel zone and the actual field at the receiver is found by retaining only one-half that obtained using only the first Fresnel zone.

A very important simplification eliminates the need for summing the

microstructure scattering effects along the path length by making use of the symmetries involved. Consider a rain cell of width $\Delta\ell$ positioned arbitrarily along the path as shown in Figure 2. The results may be stated in the form of a theorem.

The Translocation Theorem: The field intensity at the receiver is independent of the actual position of a rain cell of width $\Delta\ell$ occurring along a propagation path. It depends only on the cell width.

Proof: We need to consider the transverse extent of the rain cell only out to the edge of the first Fresnel zone. The radius of the first Fresnel zone is the locus of points for which the phase lag relative to the line-of-sight path is π radians. The total path length between the transmitter and receiver is L, and $\Delta\ell$ is an elemental length of path at a distance ℓ from the transmitter. The elemental volume defined by $\Delta\ell$ and the boundary of the first Fresnel zone is ΔV. There is no rain along the path outside ΔV. The radius of the first Fresnel zone at ℓ is given by [9].

$$F_1 = \sqrt{\frac{\lambda\ell(L-\ell)}{L}} \propto (\ell - \frac{\ell^2}{L})^{1/2} \qquad (1)$$

Note that in Figure 2 the vertical axis is greatly expanded in scale relative to the horizontal axis for typical communication links. Assuming spherical waves are transmitted, the incident field at the receiver, E^i_{rec}, will be inversely proportional to the path length L while the incident field at ℓ, E^i_ℓ, will be inversely proportional to ℓ. Thus

$$E^i_{rec} \propto \frac{1}{L} \text{ and } E^i_\ell \propto \frac{1}{\ell} \qquad (2)$$

The scattered field E^s_{rec} at the receiver from the raindrops in the volume ΔV is directly proportional to the total number of raindrops in ΔV. The scattered field at the receiver is also inversely proportional

to the distance from ΔV to the receiver $L-\ell$. Thus

$$E^s_{rec} \propto \frac{E^i_\ell \, \Delta V}{L-\ell} \tag{3}$$

Using (2)

$$E^s_{rec} \propto \frac{\Delta V}{\ell L - \ell^2} \tag{4}$$

But

$$\Delta V \propto F_1^2 \, \Delta \ell \tag{5}$$

Substituting (1) into (5) gives

$$\Delta V \propto \frac{1}{L} (\ell L - \ell^2) \, \Delta \ell \tag{6}$$

Using (6) into (4) results in

$$E^s_{rec} \propto \frac{\Delta \ell}{L} \tag{7}$$

We are interested in the scattered field relative to the incident field at the receiver, so we form the ratio and using (2) and (7) obtain

$$\frac{E^s_{rec}}{E^i_{rec}} \propto \Delta \ell \tag{8}$$

Hence the scattered field at the receiver (relative to the incident field) is independent of the position of a rain cell along the path and is independent of path length. It depends only on the width of the rain cell. Referring to (4) and (6) one sees that the reason for this is that the variation in the volume with position ℓ is exactly cancelled by the spatial variation of the scattered field at the receiver. Note that if rain is falling along the entire path, then $\Delta \ell = L$ and the ratio in (8) does indeed depend on the path length. This completes the proof of the theorem.

This theorem is useful for calculating the scattering in a rain-filled path. In the model we consider the effect of rain in only the first Fresnel zone, as shown in Figure 3a. To solve this problem we divide the total volume into N slabs by dividing the path length L into N equal segments of length $\Delta\ell = L/N$. The drops in each slab are placed in a plane at the center as illustrated for N = 4 in Figure 3b. Now the Translocation Theorem may be invoked. The contribution to the scattered field at the receiver is the same for each plane of drops and is independent of the actual position of the plane along the path. So we move all planes of drops to a convenient point along the path. When moving a plane of drops the number of drops must be changed to reflect the change in volume of the slab as discussed in the proof of the theorem. In Figure 3c all drops have been located at midpath. All planes are the same distance L/2 from the receiver and make equal contributions to the scattered field (since they all make equal contributions in their former positions). Therefore, all planes have the same number of drops and are identical. Thus the scattering solution may be found from a single plane of drops at midpath.

Although all planes can be moved to midpath to simplify calculations, the effects of multiple scattering from one plane to the next, when in their original positions, must be included. In other words, when an incident wave strikes a plane of drops the wave which leaves the plane contains the original field plus a scattered field which is changed in amplitude, phase, and perhaps, polarization. This field is now the incident field for the next plane of drops, and so on down the path. By the Translocation Theorem the positions of the individual planes are immaterial to cross polarization and attenuation, so free-space

phase shift in the region between the planes may be ignored. We will consider the effect of a single plane first and then the combined effect of a series of N planes.

For a single plane of drops scattering coefficients are defined in terms of the main polarization (polarization state of the wave leaving the transmit antenna) denoted with subscript 1 and a cross polarization (orthogonal to the main polarization) denoted with subscript 2. These coefficients will be the same for all planes and are defined as follows:

S_{pq} = scattered $\vec{E}$ field with polarization p produced by an incident $\vec{E}$ field with polarization q.

The scattered field at the receiver from a single plane of drops can be found by summing the scattered fields from each of the drops in the plane. As discussed previously it is necessary to consider only those drops in the first Fresnel zone if the result is multiplied by one-half. Since the angle of incidence and the angle toward the receiver from the plane are very small relative to the line-of-sight in most situations, we may use the forward scattering coefficients for a single drop f_{pq}. The scattering coefficients for a plane of drops are then of the form

$$S_{pq} = \frac{1}{2} \Sigma E_p^i f_{pq} \frac{e^{-jkr}}{r} \qquad (9)$$

where E_p^i is the electric field incident on the plane of the drops, r is the distance from the drop to the receiver, f_{pq} is the forward scattering function for a single drop from the p^{th} to the q^{th} polarization, and where the summation is performed over those drops in the first Fresnel zone. Assuming that all drops are identically oriented, then f_{pq} is constant for all drops. Also since we have assumed $F_1 << L$ we

have $r \simeq L/2$ (for planes at midpath) for the r in the denominator of (9). Thus

$$S_{pq} = \frac{E^i_p f_{pq}}{L} \Sigma e^{-jkr} \tag{10}$$

For a uniform distribution of drops within the first Fresnel zone, the summation in (10) is easily evaluated. The result is a complex constant C times the number of drops in the plane D. Hence

$$S_{pq} = \frac{E^i_p f_{pq}}{L} C D \tag{11}$$

The effect of N planes of drops in series may be found by considering the incident field to interact with the first plane producing a new field which then interacts with the second plane, etc. until all N planes have been considered. This may be expressed in closed form in terms of the scattering coefficients (S_{pq}'s). It is assumed that the incident field at midpath has amplitude two so that the incident field at the receiver has unity amplitude. It is also assumed that the contribution from the S_{21} coefficient (scatter from cross to main polarization) is small and thus S_{21} is taken to be zero. This is valid for cross polarization levels less than about -5 dB.

The total fields at the receiver are obtained by induction from the effect of a single plane. After interaction with the first plane of drops the total main polarization field E_M will consist of the sum of the incident field at the receiver (unity) and the scattered field S_{11}. The total cross polarization field E_X will consist only of the scattered field S_{12} since the incident field in this polarization is zero. The fields leaving plane 1 then interact with plane 2. The main polarization component is multiplied by another $(1 + S_{11})$ factor. The

cross polarization component from plane 2 consists of two parts. The previous cross polarized component E_X is multiplied by a $(1 + S_{22})$ factor, and also there is a new contribution from the incident E_M equal to $E_M S_{12}$. Thus the fields at the receiver after passing through two planes are

$$E_M = (1 + S_{11})^2 \tag{12}$$

and

$$E_X = S_{12} (1 + S_{11}) + S_{12} (1 + S_{22}) \tag{13}$$

To be rigorous (12) should include a term $S_{12} S_{21}$, but we have assumed S_{21} to be zero. Continuing this method for all N planes gives the following result:

$$E_M = (1 + S_{11})^N \tag{14}$$

$$E_X = S_{12} [(1 + S_{22})^{N-1} + (1 + S_{22})^{N-2} (1 + S_{11}) + \ldots\ldots\ldots + (1 + S_{22})(1 + S_{11})^{N-2} + (1 + S_{11})^{N-1}] \tag{15}$$

Evaluation of E_M and E_X for rain is discussed in the next section, but the development presented here is applicable to any population of scatterers. To use it one must know the scattering properties of an individual scatterer and the size, shape, and orientation distributions of the overall population.

APPLICATIONS OF THE MODEL

In this section the evaluation of the scattering coefficients presented in the previous section will be discussed for rain. Then the expressions for the received electric field intensities in (14) and (15) can be evaluated. The results of several examples will then

be given. This will demonstrate the usefulness of the model and also allow comparison to previous models and experimental results.

Calculation of the scattering coefficients from (10) requires the evaluation of two factors, f_{pq} and $\Sigma\, e^{-jkr}$. The f_{pq} factor is the forward scattering function for a single rain drop from the p^{th} to the q^{th} polarization. This is the most difficult aspect of the model. Recently, Oguchi [10] has solved for the scattering properties of oblate rain drops encountered in real rains for the frequencies of 19.3 and 34.8 GHz. He used three different techniques to solve for the forward and backward scattering of a single drop when illuminated by polarizations parallel to the drop minor axis (vertical polarization) and parallel to the drop major axis (horizontal polarization). Using these results one may determine f_{pq} through some simple geometric relationships. If Θ is the angle between the incident linear polarization (polarization 1) and the vertical we find

$$\begin{aligned} f_{11} &= f_v \cos^2 \Theta + f_h \sin^2 \Theta \\ f_{22} &= f_v \sin^2 \Theta + f_h \cos^2 \Theta \\ f_{12} &= (f_v - f_h) \sin \Theta \cos \Theta = - f_{21} \end{aligned} \tag{16}$$

where f_v is the ratio of the scattered electric field intensity from the drop which is vertically polarized to the incident vertically polarized field and f_h is the ratio of the scattered electric field intensity from the drop which is horizontally polarized to the incident horizontally polarized field.

The factor $\Sigma\, e^{-jkr}$ is the summation over all drops which have been moved to the mid-path plane, extending out a distance F_1 from the line-of-sight path. This accounts for the phase differences of the scattered

waves from each drop. Letting ρ be the radial distance from the line-of-sight path we may write

$$\Sigma\ e^{-jkr} \approx \Sigma\ e^{-j\frac{2k}{L}\rho^2} \tag{17}$$

since $L/2 >> \rho$. Here the phase shift along the line-of-sight path has been removed; the total phase shift involves a -jkL term added to the exponent. Note that for $\rho = F_1$ the phase lag under the summation sign is $-\pi$, as it should be at the first Fresnel radius. The summation can now be carried out by dividing the plane into M rings. The rings will contain an equal number of drops if the radial distance to the center of each ring is

$$\rho_m = \sqrt{m-1/2}\,\frac{F_1}{\sqrt{M}} \qquad 1 \leq m \leq M. \tag{18}$$

Substituting (18) into (17) and summing over M rings, each with D/M number of drops, gives

$$\Sigma\ e^{-jkr} = \frac{D}{M}\sum_{m=1}^{M} e^{-j\frac{\pi}{M}(m-1/2)} \tag{19}$$

This series is easily summed, giving

$$\Sigma\ e^{-jkr} = \frac{D}{M}\,\frac{2\ e^{-j2\ \pi/M}}{1-e^{-j\ \pi/M}} \tag{20}$$

Letting M approach infinity we obtain

$$\Sigma\ e^{-jkr} \approx (-j\,\frac{2}{\pi})D \tag{21}$$

We can identify the complex constant C in (11) as

$$C = -j\,\frac{2}{\pi} \tag{22}$$

The scattering coefficients by (11) may now be calculated using

the f_{pq} in (16) and (22). These are then used to compute the received field intensities in the main and cross polarized states from (14) and (15). The number of slabs, N, should be large enough to obtain convergence. Typically this number is about 200 (convergence to within 10% is obtained for N = 20), and the calculations require less than ten seconds of computer time on an IBM 370/155.

There are several results which may be obtained from calculations using this model. First, the attenuation due to rainfall is found as follows

$$A = 20 \log (|E_M|) \text{ dB} . \tag{23}$$

Recall that the incident field at the receiver without rainfall would be unity so that it is unnecessary to divide E_M by E^i_{rec}. The attenuation as a function of rain rate for a one kilometer path is plotted in Figure 4 for a frequency of 19.3 GHz. Included for comparison are the results based on differential attenuation from Oguchi [10]. The two models are in close agreement. In Figure 5 is shown the differential phase shift at 19.3 GHz for a one kilometer path. This is the amount that the phase of the received signal for a vertically polarized transmitted wave leads the received signal phase when a horizontally polarized wave is transmitted. Shown for comparison are the results of Oguchi [10] and Morrison, et.al., [11]. The agreement is not as good as was obtained for attenuation, but there is no experimental data to support any of the curves.

Another important application of the model is the calculation of cross polarization level

$$XPOL = 20 \log (|E_X|/|E_M|) \text{ dB} . \tag{24}$$

This is also available from Watson's method [5] using Oguchi's differential attenuation and differential phase shift values [10] for 100% oblate drops. Figure 6 presents a comparison of the cross-polarization level as a function of rain rate for a 1 Km path at 19.3 GHz and waves linearly polarized at 45° with respect to the drop axis. The agreement is quite close and for the first time presents an independent theoretical confirmation of the differential attenuation-differential phase shift approach.

The percentage of oblate drops is somewhat difficult to manipulate in the differential attenuation-differential phase shift model, and for this reason it has been kept at 100%, but it is doubtful that this is the correct value.

Jones [8] has found that real rain consists of 32% spherical, 28% oblate spheroidal, 18.5% prolate spheroidal, and 21.5% irregular shaped drops, for drops greater than 1.9 mm equivalent spherical diameter. All drop shapes except spherical could contribute to the cross-polarization level. About one-half of the prolate drops would be expected to be aligned with their elliptical cross-section facing the incident field and, therefore, producing depolarization. This would increase the effective percentage of oblate drops to about 37%. Since the irregular shaped drops would provide a small but unknown contribution, the effective percentage of oblate drops is fixed at 40% for this analysis. An increase of 5% in this number yields an increase of about 1 dB in the cross-polarization. The effective percentage of oblate drops is included in the calculations by weighting S_{12} by a factor $P(0 \leq P \leq 1)$ which represents the fraction of the

drops which have the oblate shape. S_{11} and S_{22} are each the sum of two terms: one term calculated using the f_{pp} for spherical drops and weighted by the percentage of spherical drops, and the other term calculated using the f_{pp} for oblate drops and weighted by the percentage of oblate drops. Previous models have assumed that all drops have the same oblate shape.

Figure 6 displays the expected cross-polarization level for a 1 Km path at 19.3 GHz with 45° linear polarization incident on a rain-filled volume with 40% oblate drops. This curve is significantly lower than the curve for 100% oblate drops. It also is in much better agreement with published data [12].

A further application of the model is calculation of the cross-polarization generated by rain as a function of the tilt angle of the input linear polarization. See Figure 7. The angle θ is the angle between the electric field vector and the drop minor axis. For no canting angle $\theta = 0°$ would be vertical polarization. The curves in Figure 7 are for 1 and 5 Km paths at 100 mm/hr. rain rate. The cross-polarization response of a rain-filled path 1 Km long is nearly symmetrical about $\theta = 45°$. For longer paths, such as the 5 Km path shown, the cross-polarization level maximizes nearer to $\theta = 90°$ than $\theta = 0°$. This has not been reported in the literature. In fact, the statement that the response is symmetric about $\theta = 45°$ is frequently made. This result has important consequences. Since the drop canting angle may vary about $\pm 15°$ from its nominal position of major axis parallel to the ground, a horizontally polarized wave has a θ from 75 to 90° and a vertically polarized wave has θ from 15 to 0°. From the L = 5 Km curve of Figure 7 a 15° canting angle gives rise to -18 dB cross-polarization

for vertical polarization and -9 dB for horizontal polarization. Thus, horizontally polarized waves are much more sensitive to depolarization due to rain drop canting than are vertically polarized waves, and the peak of the cross-polarization level shifts toward $\theta = 90°$ with increasing path length. Also, for experiments with dual orthogonal, linear polarizations horizontal and vertical polarizations are likely to have a wide scatter of the data about the expected result because of the changing distribution of canting angles in real rains. This makes a comparison with theory difficult. With $\pm 45°$ linear polarizations for, say, a 1 Km path the change in cross-polarization due to changes in θ (due to canting angle changes) is small and an accurate comparison with theory is possible. This result agrees with an experiment performed by Shimba [13] who measured a cross-polarization level of -10 dB for a 4.3 Km path, a 140 mm/hr. rain rate, and a frequency of 19.1 GHz. The input polarization was horizontal and the high value of cross-polarization is easily explained using these ideas and assuming a small non-zero canting angle of the drops.

The new model of depolarization has been developed here only for linear polarizations transmitted. Coupling the model with the general theory of depolarization as given by Beckmann [14] one can obtain the depolarization by rain for an arbitrarily polarized wave. We can do this if the depolarization of two orthogonal linearly polarized waves is known. These, of course, can be found from the model.

CONCLUSIONS

The model presented here provides a means for calculating precipitation depolarization and attenuation which is independent

of van de Hulst's equivalent refractive index and of the differential attenuation-differential phase shift concept. It can be applied to propagation through precipitation which has no axes of symmetry or preferred polarizations. Since all of the important parameters are explicit rather than implicit, it provides a rapid means for analyzing propagation through rain under arbitrary distributions of drop shapes and sizes.

REFERENCES

[1] D. C. Hogg, "Millimeter-wave communication through the atmosphere," Science, Vol. 159, pp. 39-46, 5 January 1968.

[2] T. Oguchi, "Attenuation of electromagnetic waves due to rain with distorted raindrops," J. Radio Res. Lab., Jap., Vol. 7, pp. 467-485, September 1960.

[3] _____, "Attenuation of electromagnetic waves due to rain with distorted drops," J. Radio Res. Lab., Jap., Vol. 11, pp. 19-44, January 1964.

[4] D. T. Thomas, "Cross polarization distortion in microwave radio transmission due to rain," Radio Science, Vol. 6, pp. 833-840, October 1971.

[5] P. A. Watson and M. Arbabi, "Rainfall cross polarization at microwave frequencies," Proc. IEE (London), Vol. 120, April 1973.

[6] H. C. van de Hulst, Light Scattering by Small Particles, New York: John Wiley Sons, Inc., 1957, pp. 28-34.

[7] J. O. Laws and D. A. Parsons, "The relation of raindrop-size to intensity," Trans. Am. Geophysical Union, Vol. 24, pp. 432-460, 1943.

[8] D. M. A. Jones, "The shape of raindrops," Journal of Meteorology, Vol. 16, pp. 504-510, October 1959.

[9] D. C. Livingston, The Physics of Microwave Propagation, Englewood Cliffs, New Jersey: Prentice-Hall, 1970, Chapter 3.

[10] T. Oguchi, "Attenuation and phase rotation of radio waves due to rain: Calculations at 19.3 and 34.8 GHz," Radio Science, Vol. 8, pp. 31-38, January 1973.

[11] J. A. Morrison, M. J. Cross, and T. S. Chu, "Rain-induced differential attenuation and differential phase shift at microwave frequencies," Bell System Technical Journal, Vol. 52, pp. 599-604, April 1973.

[12] C. W. Bostian, W. L. Stutzman, P. H. Wiley, and R. E. Marshall, "Initial results of an experimental study of 17.65 GHz rain attenuation and depolarization," IEEE G-AP International Symposium Digest, pp. 250-253, December 1972.

[13] M. Shimba and K. Morita, "Radio propagation characteristics due to rain at 19 GHz," 1972 G-AP International Symposium Digest, pp. 246-249, December 1972.

[14] P. Beckmann, The Depolarization of Electromagnetic Waves, Boulder, Colorado: The Golem Press, 1968, pp. 39-41.

LIST OF CAPTIONS

Figure 1. Depolarization by differential attenuation.

Figure 2. Geometry used in proof of theorem.

Figure 3. Division of path when N = 4.

Figure 4. Attenuation versus rain rate for a 1 km path at 19.3 GHz.

Figure 5. Differential phase shift (vertical minus horizontal) for a 1 km path at 19.3 GHz versus rain rate.

Figure 6. Cross polarization level versus rain rate for a path length of 1 km and a rain drop canting angle of 45° at 19.3 GHz.

Figure 7. Cross polarization level versus Θ, the angle between the electric field vector for a linearly polarized wave and the minor axis of the raindrops, for path lengths of 1 and 5 km and a frequency of 19.3 GHz and a rain rate of 100 mm/hr.

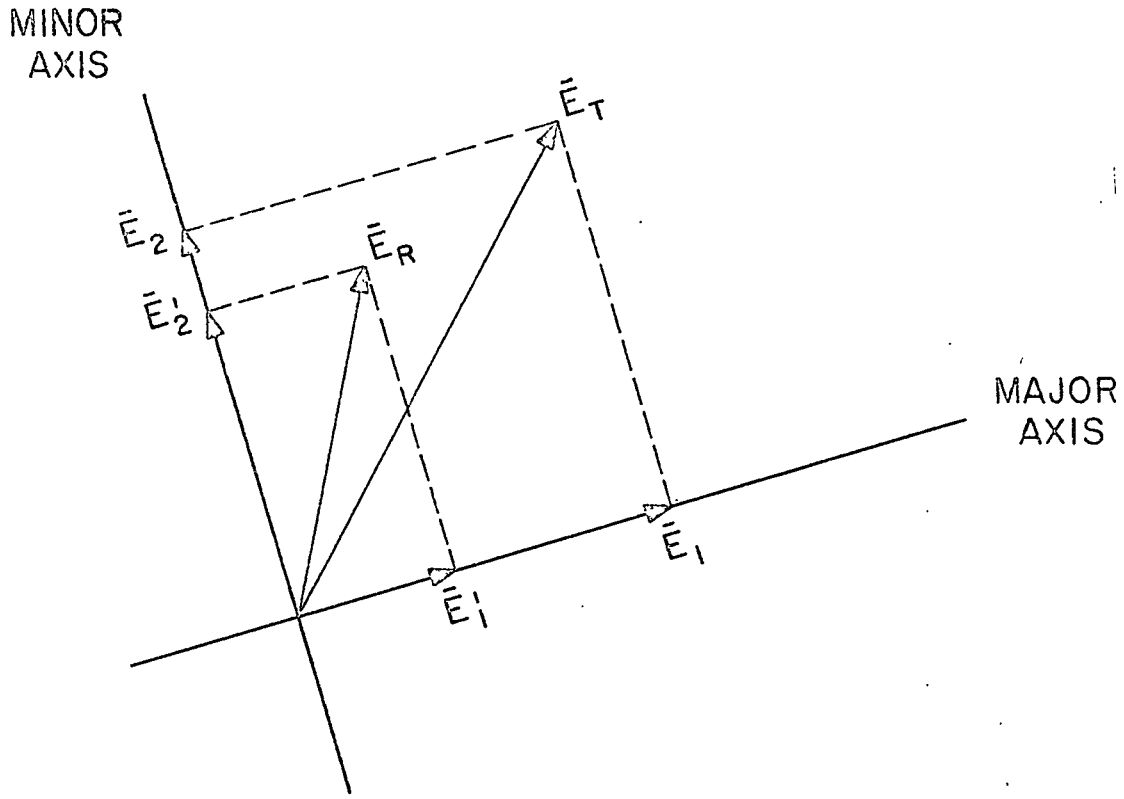

Fig. 1

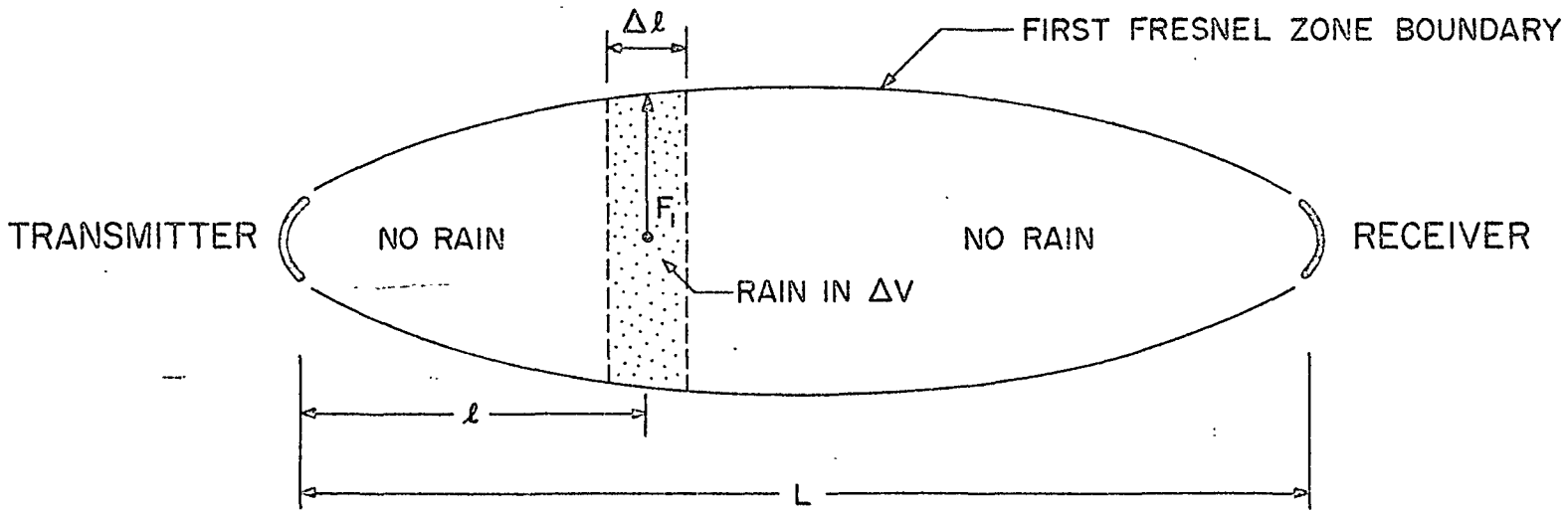
Δℓ
FIRST FRESNEL ZONE BOUNDARY
TRANSMITTER
NO RAIN
F1
NO RAIN
RECEIVER
RAIN IN ΔV
ℓ
L

Fig. 2

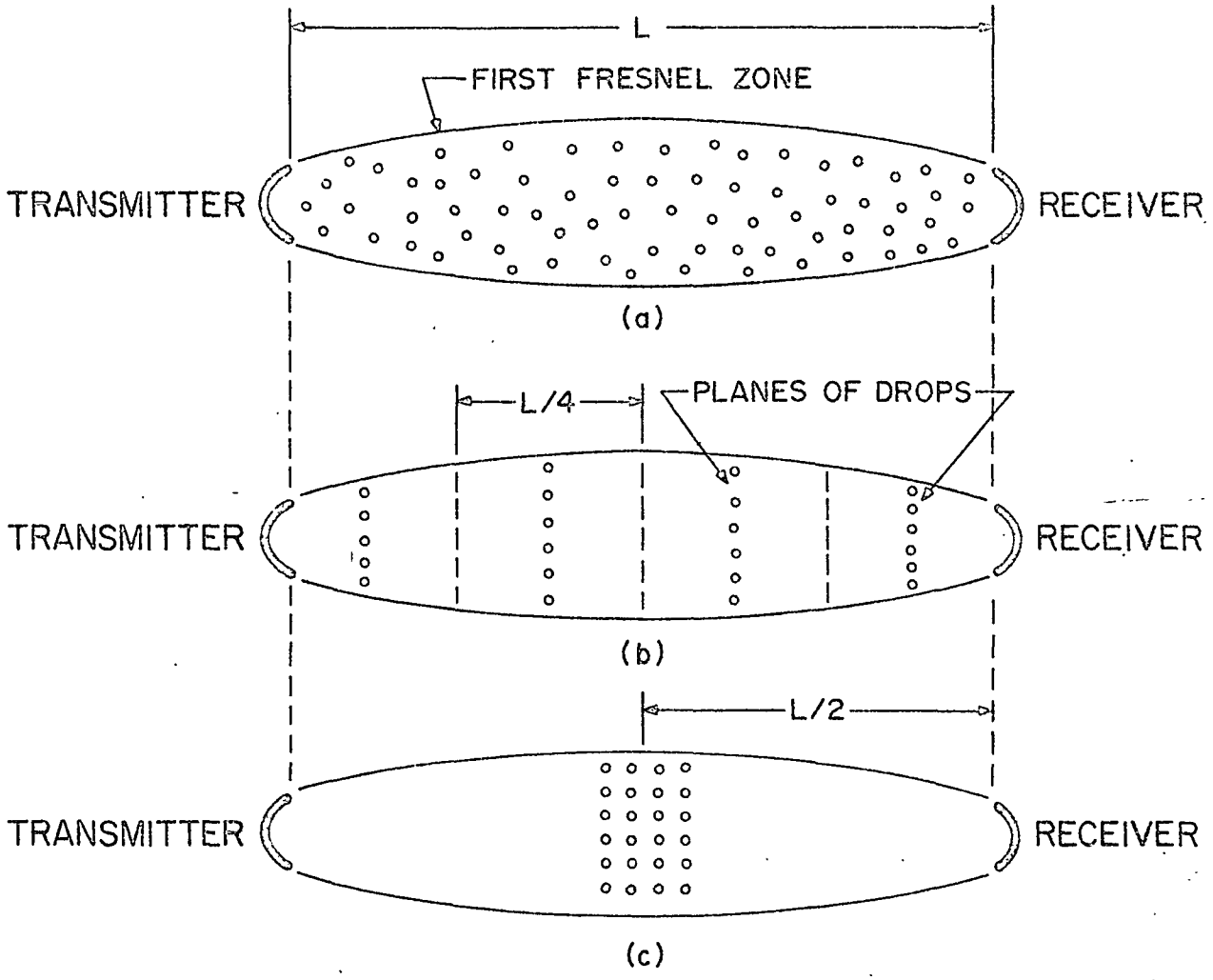
L
FIRST FRESNEL ZONE
TRANSMITTER
RECEIVER
(a)
L/4
PLANES OF DROPS
TRANSMITTER
RECEIVER
(b)
L/2
TRANSMITTER
RECEIVER
(c)

Fig. 3

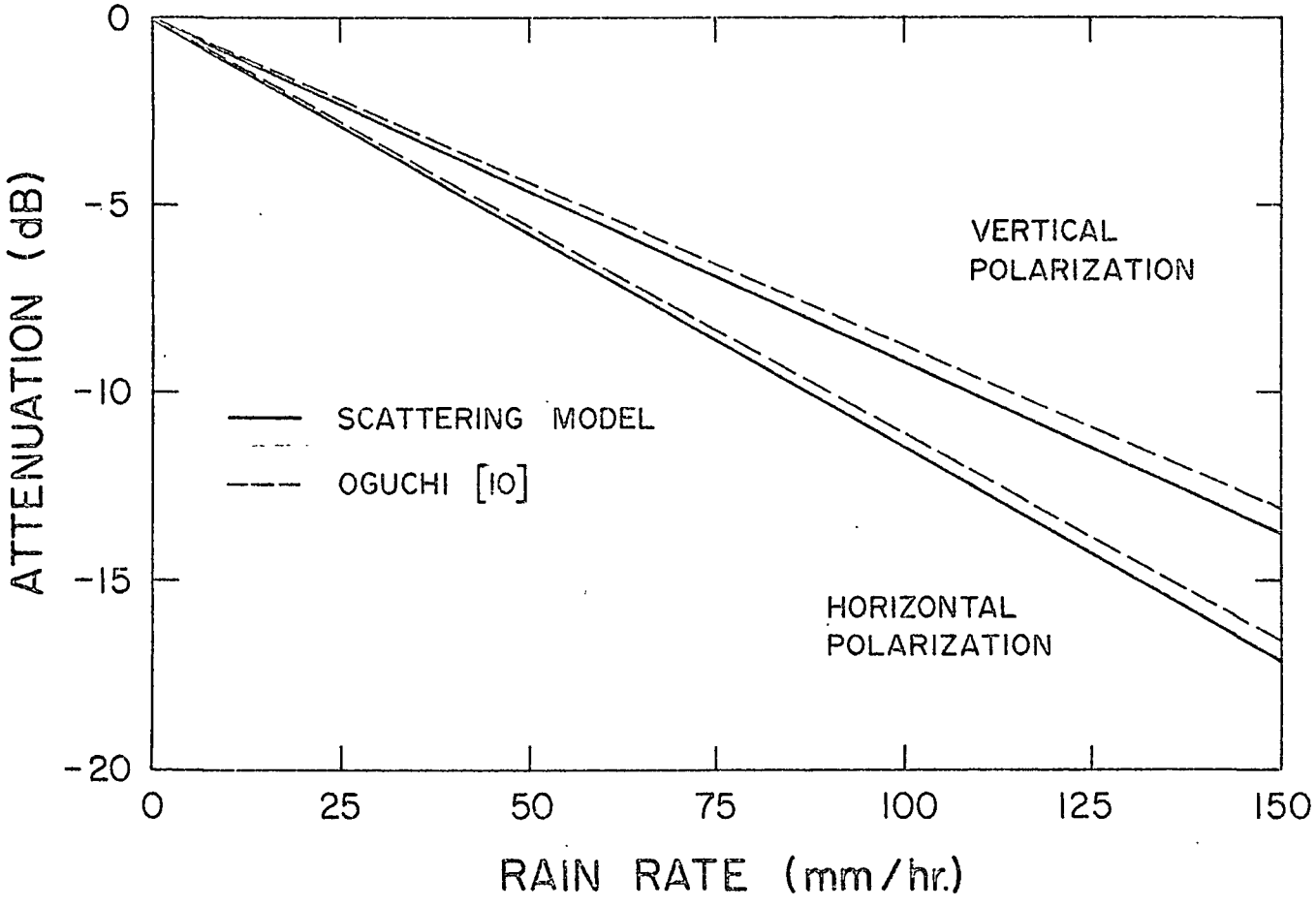
0
-5
-10
-15
-20
ATTENUATION (dB)
0
25
50
75
100
125
150
RAIN RATE (mm/hr.)
VERTICAL
POLARIZATION
HORIZONTAL
POLARIZATION
SCATTERING MODEL
OGUCHI [10]

Fig. 4

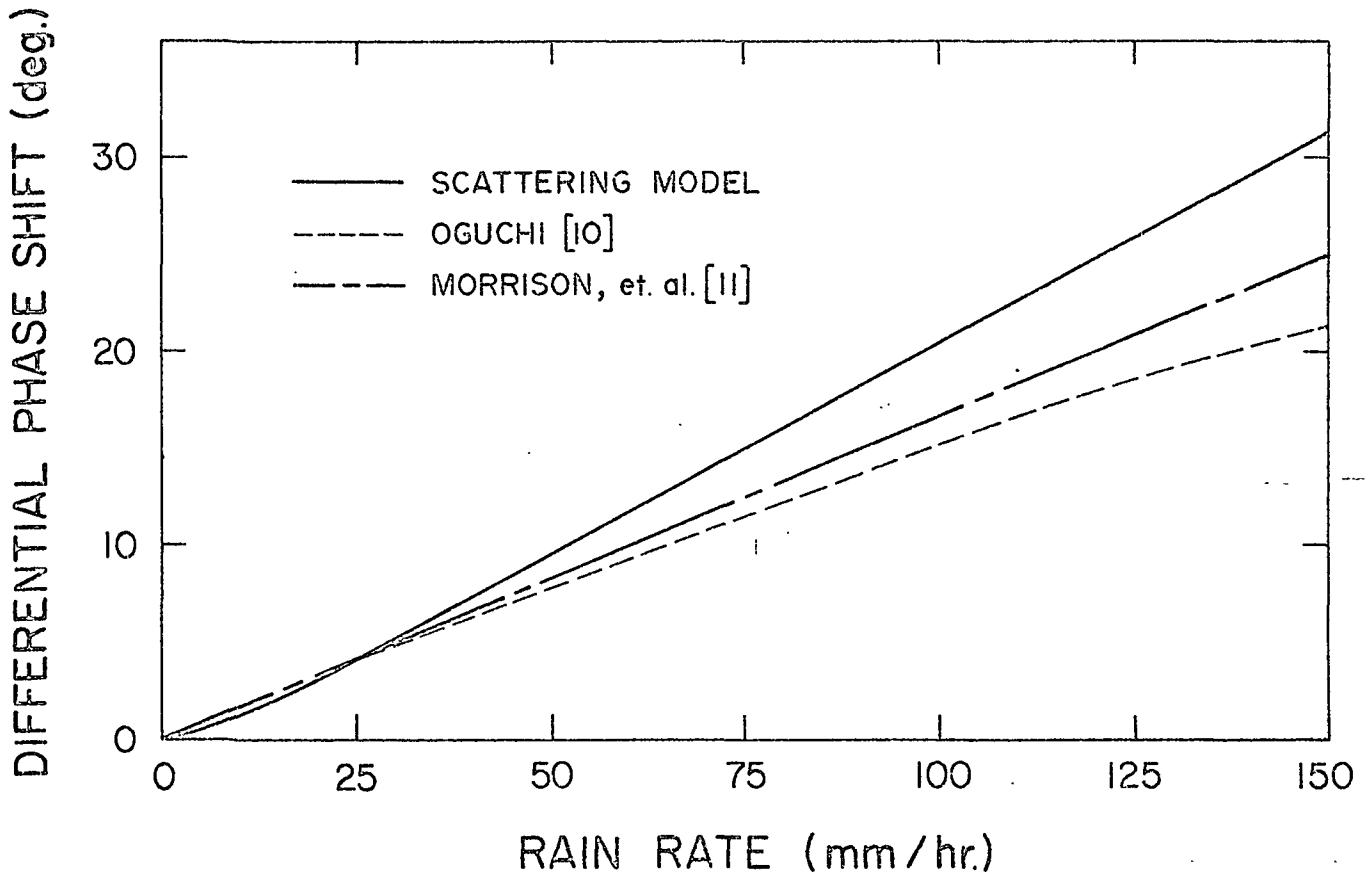
DIFFERENTIAL PHASE SHIFT (deg.)
30
20
10
0
SCATTERING MODEL
OGUCHI [10]
MORRISON, et. al. [11]
0
25
50
75
100
125
150
RAIN RATE (mm/hr.)

Fig. 5

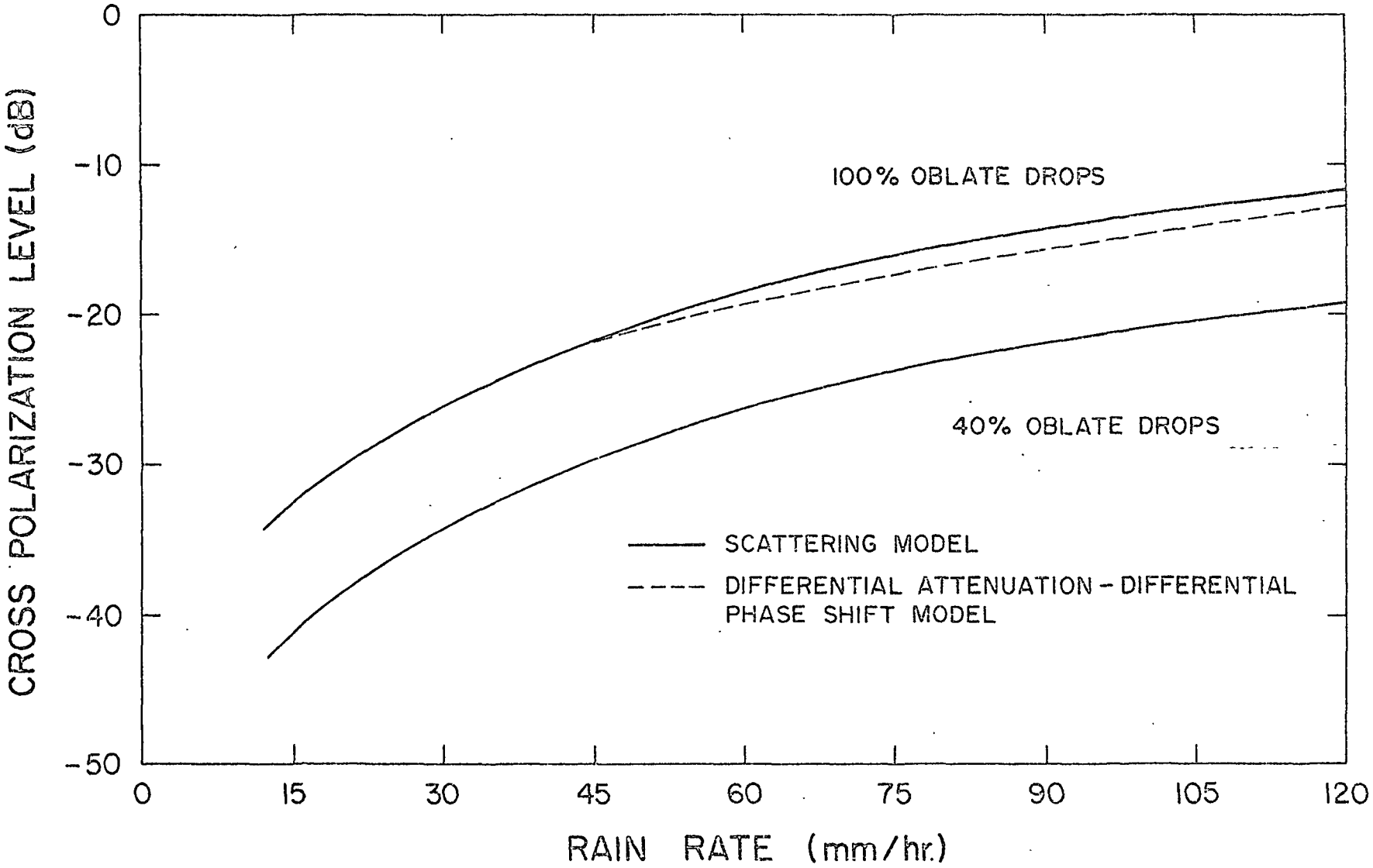
CROSS POLARIZATION LEVEL (dB)
0
-10
-20
-30
-40
-50
0
15
30
45
60
75
90
105
120
RAIN RATE (mm/hr.)
100% OBLATE DROPS
40% OBLATE DROPS
SCATTERING MODEL
DIFFERENTIAL ATTENUATION - DIFFERENTIAL PHASE SHIFT MODEL

Fig. 6

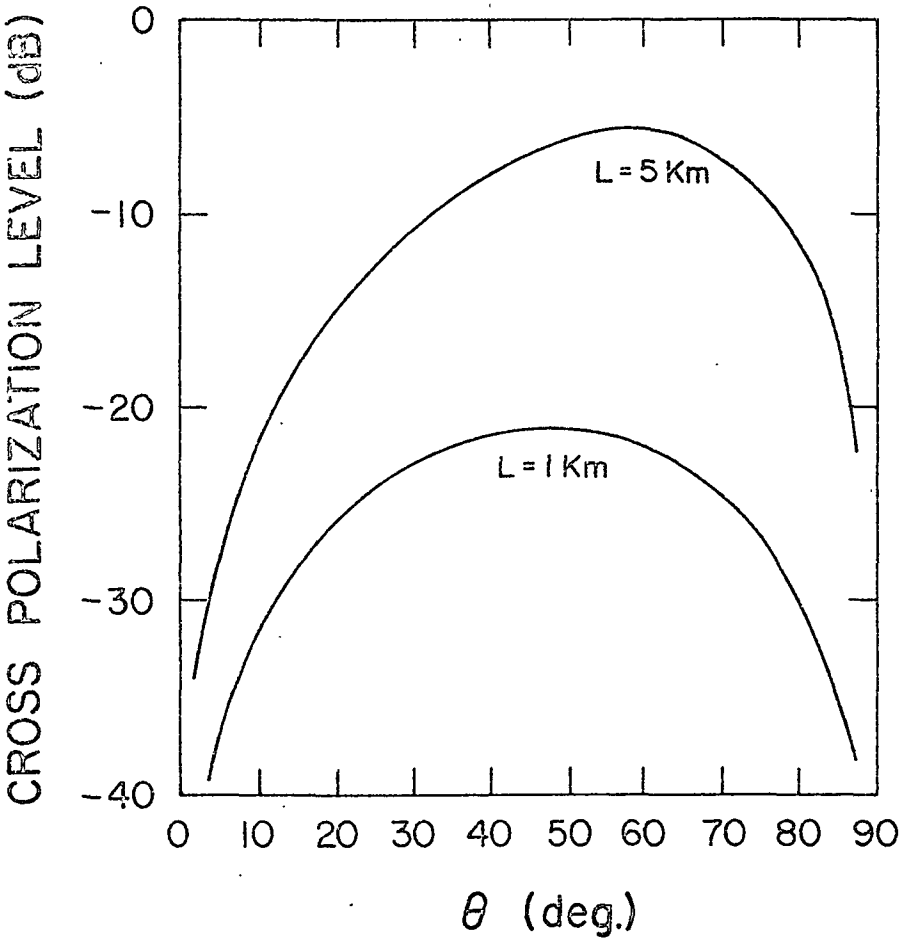
CROSS POLARIZATION LEVEL (dB)
0
-10
-20
-30
-40
L = 5 Km
L = 1 Km
0
10
20
30
40
50
60
70
80
90
θ (deg.)

Fig. 7